WILEY SURFACE and INTERFACE ANALYSIS

Investigation of work function and chemical composition of thin films of borides and nitrides

A. Mezzi[1] | P. Soltani[1] | S. Kaciulis[1] | A. Bellucci[2] | M. Girolami[2] | M. Mastellone[2] | D. M. Trucchi[2]

[1] ISMN-CNR, PO Box 10, 00015 Monterotondo Stazione, Rome, Italy

[2] ISM-CNR, PO Box 10, 00015 Monterotondo Stazione, Rome, Italy

Correspondence
A. Mezzi, ISMN-CNR, PO Box 10, 00015 Monterotondo Stazione, Rome, Italy.
Email: alessio.mezzi@ismn.cnr.it; alessio.mezzi@gmail.com

Thin films of various borides, nitrides, and barium fluorides were tentatively deposited by pulsed laser deposition and by magnetron sputtering in order to develop the components of thermionic-photovoltaic devices for the high-temperature thermal to electrical conversion by solid state. To improve the device performance, the materials characterized by a low work function were selected. In the present work, the chemical composition and work function of obtained films were investigated by X-ray photoelectron spectroscopy and ultraviolet photoelectron spectroscopy techniques. The values of work function were determined from the cut-off in the He I valence band spectra. Different films were compared and estimated on the basis of X-ray photoelectron spectroscopy and ultraviolet photoelectron spectroscopy results.

KEYWORDS

borides, nitrides, thermionic-photovoltaic, UPS, work function

1 | INTRODUCTION

The rapid development of the new technologies and global world economy is remarkably accompanied by exponential increase of the energy demand. In 2010, it was predicted the growth by 56% till 2040.[1] However, the conventional energy sources based on fossil fuel resources are limited and strongly dangerous for our environment.[2] For this reason, many research activities in the last decades have been addressed to the renewable energy technologies and eco-friendly energy sources, identified as a good alternative. In particular, the solar radiation is commonly considered as an abundant, cheap, clean, and sustainable energy source. However, the performances of solar energy converters to date are still less competitive than the conventional power generators. One of the best solution to improve their performances could be the development of renewable energy sources based on hybrid systems, offering advantages in terms of cost, reliability, and efficiency.[3,4] In this context, the solid-state devices like thermionic-photovoltaic (TIPV) converters have been proposed for the conversion of concentrated solar energy. In general, thermionic converters are experiencing an increasing interest if integrated with solar

concentrations.[5] TIPV converters consist of 3 main elements: electron emitter (cathode), collector (anode), and thermophotovoltaic (TPV) cell.[6] The main characteristics of the emitter are the enhanced capability to emit electrons and the selective thermal emittance, which should be able to satisfy the specific requirements of the PV cell in terms of radiation absorption. Basically, an ideal cathode must have a low work function ϕ_c, in order to emit a large amount of electrons, but it must be higher than that of anode ϕ_a in order to allow the collection of electrons guaranteeing a correct output voltage.

In the present work, thin films of various borides and nitrides were deposited by pulsed laser deposition (PLD), a versatile technique for the controlled deposition of nanostructured films of numerous materials on various substrates,[7] with an aim to improve the cathode and anode performances in TIPV devices. The thermionic electron emission properties of lanthanum hexaboride (LaB_6) and cerium hexaboride (CeB_6) films are well established. For this reason, they were considered as good candidates in terms of low work function (ϕ = 2.5-2.6 eV) and high melting point (T_m > 2000°C).[8,9] Another valid alternative could be represented by nitride films, in particular, the amorphous carbon nitride (CN_x) and hydrogenated aluminium nitride (AlN:H), because

their work function can be even lower.[10,11] In the TIPV, the cell could play itself the role of thermoionic anode. GaAs was selected for the development of the TPV cell, but it is characterized by ϕ = 4.6 eV for p-type; thus, it could not provide the necessary condition $\phi_c > \phi_a$. Therefore, its work function was tentatively reduced with an ultra-thin film of BaF_2, deposited by RF magnetron sputtering. The aim of the present work was the exploration by using X-ray photoelectron spectroscopy (XPS) and ultraviolet photoelectron spectroscopy (UPS) techniques, how the surface chemical composition and work function depend on different growth parameters. The work function ϕ was calculated by using the formula: $\phi = h\nu$ (He I) − E_{cutoff}, where E_{cutoff} is the energy of the cut-off level in the valence band spectrum excited by He I line.[12] In order to avoid the low kinetic energy cut-off caused by the spectrometer, the work function ϕ was measured following the method proposed by Martinez et al,[12] developed to determine the influence of a negative bias (V) on the potential barrier at insulator-vacuum surface. This method consists in the acquisition of UPS spectra applying a series of negative bias voltages V. Because the photoemission threshold linearly depends on the square root of the absolute value of negative bias applied to the sample, as described by the classical Schottky model for a potential barrier, the work function value was calculated from the plot of E_{cutoff} = f($\left| V \right|^{1/2}$).

2 | EXPERIMENTAL

2.1 | Sample preparation

Thin films of borides (samples LB1, LB2, LB3, and CeB) and nitrides (samples AlN1, AlN2, AlN3, and CN) were deposited onto Si and SiO_2/Si substrates by PLD, equipped with an ArF excimer laser (Lambda Physik COMPex 102) operating at 193-nm wavelength and 7-ns pulse duration. The commercial targets of LaB_6, CeB_6, AlN, and C (purity 99.95 wt%) were employed for the deposition. The pulse deposition rate was kept constant at 10 Hz, whereas the energy pulse was 80 mJ for borides and 60 mJ for nitrides. Carbon nitride films were grown by RF plasma assisted PLD,[13] in a reactive atmosphere of N_2/Ar flux (16/32 sccm) with a rf power of 20 W. Deposition temperatures, operating pressure, and time are listed in Table 1.

TABLE 1 Deposition parameters (T_{dep}, pressure P and deposition time t), surface chemical composition, and work function ϕ of the investigated samples

Sample	T_{dep}, °C	P, mbar	t, min	B 1s	La $3d_{5/2}$	C 1s	O 1s	Si 2p	La/B	ϕ, eV	d, nm
LB1	400	2.8×10^{-6}	180	21.3	8.6	24.8	44	1.4	0.4	3.3	6.0
				After 30 s of ion sputtering							
				23.6	14.2	9.9	49.4	3.0	0.6	3.4	
LB2	500	2.8×10^{-6}	240	16.1	5.2	36.0	42.3	0.4	0.3	3.4	8.7
				After 30 s of ion sputtering							
				19.8	11.0	17.8	49.5	1.8	0.6	3.3	
LB3	500	8.7×10^{-7}	90	8.9	4.5	47.3	30	9.3	0.5	2.8	5.0
				After 30 s of ion sputtering							
				14.8	11.9	12.8	39.87	20.7	0.8	3.0	

	T_{dep}, °C	P, mbar	t, min	B 1s	Ce $3d_{5/2}$	C 1s	O 1s		Ce/B	ϕ, eV	d, nm
CB	500	2.5×10^{-6}	270	19.8	6.7	30.5	43		0.34	3.4	17.0
				After 30 s of ion sputtering							
				26.1	14.2	14.1	45.7		0.54	3.4	
				After 90 s of ion sputtering							
				26.4	17.5	13.1	43.1		0.66	3.1	

	T_{dep}, °C	P, mbar	t, min	Al 2p	C 1s	N 1s	O 1s	Si 2p	Al/N ratio	ϕ, eV	d, nm
AlN1	500	5.3×10^{-6}	45	20.6	12.8	4.6	45.4	16.7	4.5	3.3	1.6
				After 30 s of ion sputtering							
				26.7	1.1	4.6	46.3	21.3	5.8	3.0	
AlN2	400	3.3×10^{-6}	45	19.8	12.9	2.1	44.8	20.5	9.4	3.3	1.3
				After 30 s of ion sputtering							
				23.9	1.1	2.2	49.5	23.4	11.6	3.3	
AlN3	600	6.7×10^{-6}	45	21.3	12.2	3.6	41.6	21.6	5.9	3.1	1.4
				After 30 s of ion sputtering							
				25.2	1.1	4.0	45.8	23.9	6.3	2.8	

	T_{dep}, °C	P, mbar	t, min	C 1s	N 1s	O 1s	Si 2p		C/N ratio	ϕ, eV	d, nm
CN	350	4.3×10^{-1}	45	7.9	1.3	47.7	43.2		6.1	4.0	0.3

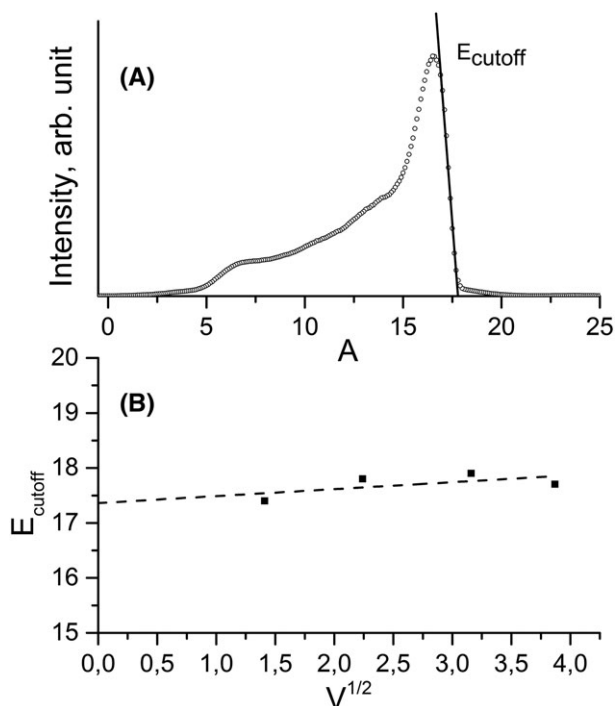|	T_{dep}, °C	P, mbar	t, min	Ba$3d_{5/2}$	F 1s	As2p3	Ga2p3	O1s	C 1s	Ba/F ratio	ϕ, eV	d, nm
BF1	RT	1.7×10^{-2}	100	13.1	22.8	2.8	17.3	29.6	14.4	0.6	3.4	0.5
				After 30 s of ion sputtering								
				6.1	2.9	30.7	39.6	20.7	–	2.1	3.5	
BF2	RT	1.7×10^{-2}	200	27.7	34.3	1.2	8.0	23.4	5.4	0.8	3.5	0.8
				After 30 s of ion sputtering								
				16.3	7.6	13.9	33.8	28.3		2.1	3.4	
BF3	RT	1.7×10^{-2}	300	27.2	31.7	0.8	2.7	20.5	17.1	0.9	3.5	2.0
				After 30 s of ion sputtering								
				25.3	14.3	11.4	21.7	27.3		1.8	3.4	

FIGURE 1 UPS spectrum of the target LaB6 (A) and the plot Ecutoff vs |V|^(1/2) (B)

The thin films of fluorides (samples BF1, BF2, and BF3) were deposited by RF magnetron sputtering. The chamber was evacuated to 1.5×10^{-6} mbar and back-filled with Ar flux to 1.7×10^{-2} mbar.

The RF power input to the BaF_2 target was kept constant at 100 W, with a negative substrate bias of 375 V with respect to ground. The substrate holder rotated during the deposition at a speed of 60 rpm, whereas the deposition time varied from 100 to 300 seconds.

2.2 | Surface characterization

The surface analyses were carried out by using an ESCALAB 250Xi (Thermo Fisher Scientific, UK), equipped with a monochromatic Al Kα source for XPS, an ultraviolet He (I and II lines) lamp for UPS and a 6-channeltron spectroscopic detection system. XPS/UPS measurements were carried out at 90° take-off angle and electrostatic or electromagnetic lens mode, resulting in 1-mm diameter of analyzed sample area. The samples were fixed on the standard sample stage by using metallic clips, guaranteeing the electrical contact between the films and the apparatus ground.

The XPS investigations were performed at a pressure of approximately $1-5 \times 10^{-9}$ mbar in the analysis chamber, which was increased up to 1×10^{-7} mbar during the ion sputtering with an ion gun EX06, which was set to 1 keV and sample current of 3 μA to limit the possible degradation of the samples. At these experimental conditions, the sputtering rate was approximately 0.11 nm/second. The spectra were collected at 20 eV constant pass energy. The binding energy (BE) scale was calibrated by positioning the C 1s peak from the surface contamination at BE = 285.0 eV with an accuracy of ±0.1 eV.
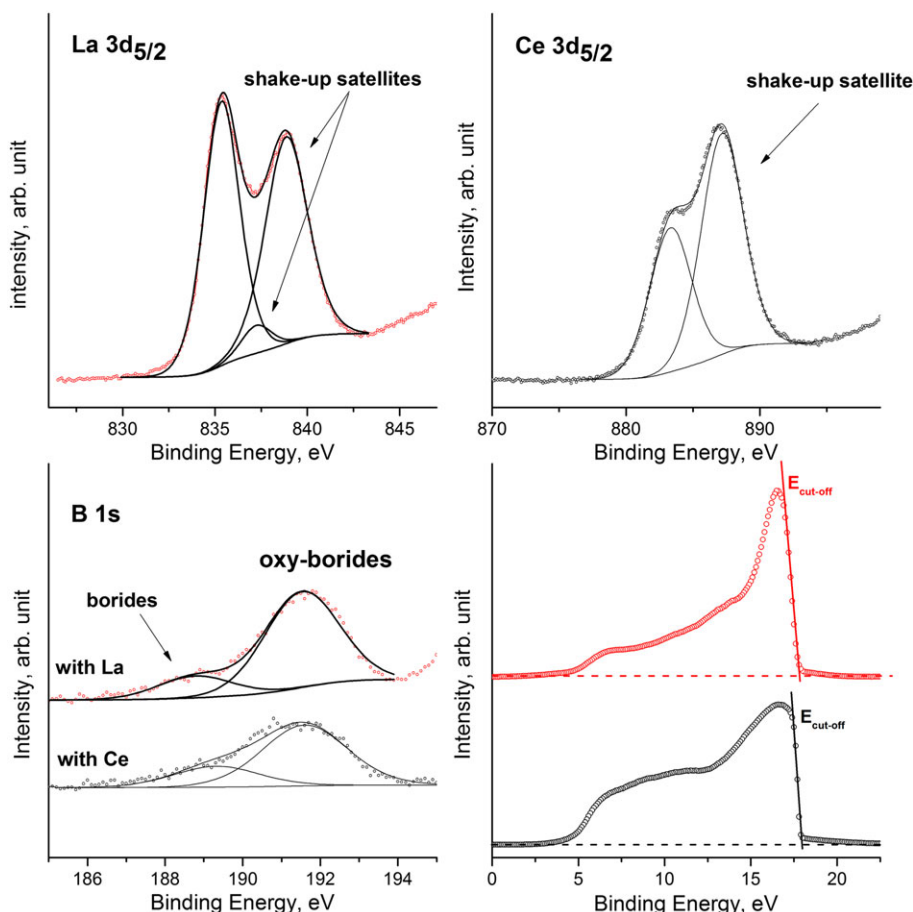

FIGURE 2 XPS and UPS (bias = 10 V) spectra of LB1 and CB samples

The UPS measurements were carried out at a pressure of approximately 2×10^{-8} and 5×10^{-9} mbar for He I and II, respectively. The spectra were collected at 2 eV pass energy. In order to check the contribution of the surface contamination, the spectra were also registered after a short surface cleaning (30 seconds) by ion sputtering. The work function ϕ of the samples was calculated by measuring the characteristic cut-off energy in the He I spectrum, as shown in Figure 1. A negative bias of 2, 5, 10, and 15 V was applied to shift the spectra from the spectrometer threshold. The E_{cutoff} values measured at different bias voltages were plotted as E_{cutoff} vs $|V|^{1/2}$ (Figure 1), as it was suggested in Martinez et al.[12] From these plots were extrapolated the values of the work function ϕ at zero bias.

Spectroscopic data were acquired and processed by the Avantage v.5 software. Shirley background subtraction and mixed Lorentzian/Gaussian peak shape (30%) were used for the peak fitting.

3 | RESULTS AND DISCUSSION

3.1 | Boride films

The obtained XPS results revealed the presence of C, O, Si, B, La, or Ce in the LB and CB samples (Table 1). C 1s signal was primarily assigned to the adventitious carbon, because it was strongly reduced after 30 seconds of ion sputtering. Si 2p signal at BE = 99.5 eV was attributed to the substrate. It was detected only in LB films, because their thickness estimated from XPS depth profile (not included) was below 10 nm. It should be noted that the absence of Si—O bond indicated the complete coverage of substrate surface. The thickness of CB sample was approximately 17 nm; therefore, the Si 2p signal from substrate was absent.

La 3d, Ce 3d, and B 1s spectra are shown in Figure 2. All these borides had a similar shape of B 1s signal, composed by 2 peaks positioned at BE = 189.3 and 192.0 eV and assigned to borides and oxy-borides, respectively.[14] The identification of La species by the peak-fitting of La 3d spectrum is complicated due to the presence of strong shake-up satellite and plasmon peaks.[15] The La $3d_{5/2}$ signal was decomposed into 3 synthetic peaks (Figure 2) positioned at BE = 835.9, 837.7, and 839.4 eV and assigned to the main peak and satellites, respectively. However, the BE value of the main peak can be attributed for either boride and oxide. Also, in the Ce 3d spectrum are present strong shake-up satellites (Figure 2). The main peak of Ce $3d_{5/2}$ was found at BE = 882.4 eV with a satellite at BE = 886.3 eV. Also, from this spectrum, it is quite complicated to discern the contribution of the oxides and borides. Therefore, the discussion of the XPS results is limited to the B 1s signal and the atomic ratios of La/B and Ce/B, focusing the main attention on the correlation between boride concentration and work function. As it is shown in the Table 1,
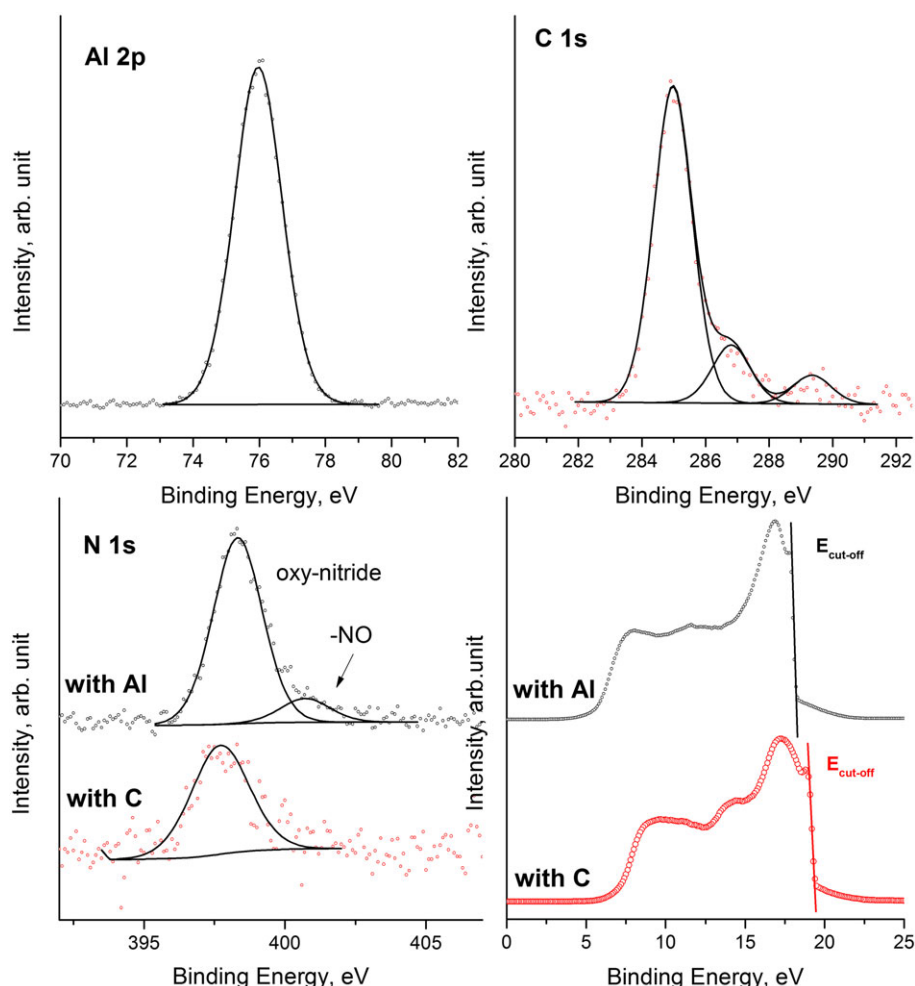

FIGURE 3 XPS and UPS (bias = 10 V) spectra of AN1 and CN samples

the La/B and Ce/B atomic ratios resulted very different from the stoichiometric one (nominal ratio 0.16). Also, after removing 0.5 nm of material by ion sputtering, a deficiency of B was still present. This can partially derive from a preferential sputtering due to the significant mass difference between La and B atoms.[15] A large content of oxygen in the bulk of all films (Figure 3) was most probably due to the favorable tendency for La oxidation.[16] As it can be expected, operating at a lower pressure (sample LB3), the oxygen content slightly decreases, but at the same time, the La/B ratio becomes worse. In any case, the different stoichiometry suggests the presence of various chemical compounds from the La—B—O and Ce—B—O family. It should be noted that the atomic ratio of the 2 species I_{boride}/I_{oxide}, calculated by the peak fitting of the B 1s signal, depends on the growth parameters. A major content of borides was found in LB3 and CB films, where I_{boride}/I_{oxide} = 0.54 and 0.49, respectively, whilst this ratio was 0.23 and 0.19 in LB1 and LB2 samples, respectively. These results can be correlated with UPS investigations, where almost all boride films, before and after sputtering, had the same work function ϕ = 3.3-3.4 eV, except of LB3 characterized by the lowest work function ϕ = 2.8-3.0 eV, before and after sputtering. This is not a surprise, because the XPS quantification evidenced a higher concentration of borides in LB3 sample. Moreover, it should be noted that after a longer sputtering (90 seconds), CB film had a lower work function ϕ = 3.0 eV. This is most probably due to the removal of the surface contaminants, because the I_{boride}/I_{oxide} ratio remained unchanged.

3.2 | Nitrides

The chemical composition of nitride films reported in Table 1 displays the presence of Al, N, O, Si, and C in AlN samples and C, N, O, and Si in CN sample. The thickness of these films was very small, approximately 1.5 nm for AlN samples and only 0.3 nm for CN sample. This result was confirmed by the presence of Si and O, which compose the substrate (Si wafer covered with a SiO_2 layer of 4.0 nm). The Si 2p signal was fitted by 2 synthetic peaks, positioned at BE = 99.5 and 103.0 eV and assigned to Si^0 and SiO_2, respectively. The presence of the underlying Si^0 confirms that a very thin nitride film was deposited.

Al 2p, C 1s, and N 1s spectra of AlN and CN samples are shown in Figure 3. From Al 2p peak in AlN samples at BE = 74.5-74.8 eV, it is impossible to identify the chemical state of Al due to the overlap of AlN and aluminium oxides.[17] However, the formation of nitride was confirmed by the N 1s peak at BE = 398.0-398.3 eV, typical for oxynitrides.[18,19] The calculated atomic ratios of Al/N (Table 1) evidenced an excess of Al that was partially oxidized. The situation was more or less the same for CN sample, where was registered a high excess of C (nominal ratio C/N = 0.75). The C 1s region was fitted by 3 synthetic peaks (Figure 3), positioned at BE = 285.0, 286.8, and 289.3 eV and assigned to C—C bond, a sp^2 C=N or C—O bonds and oxidized carbon,[20] respectively. Only a single peak at BE = 398.2 eV was registered in the N 1s spectrum, which is
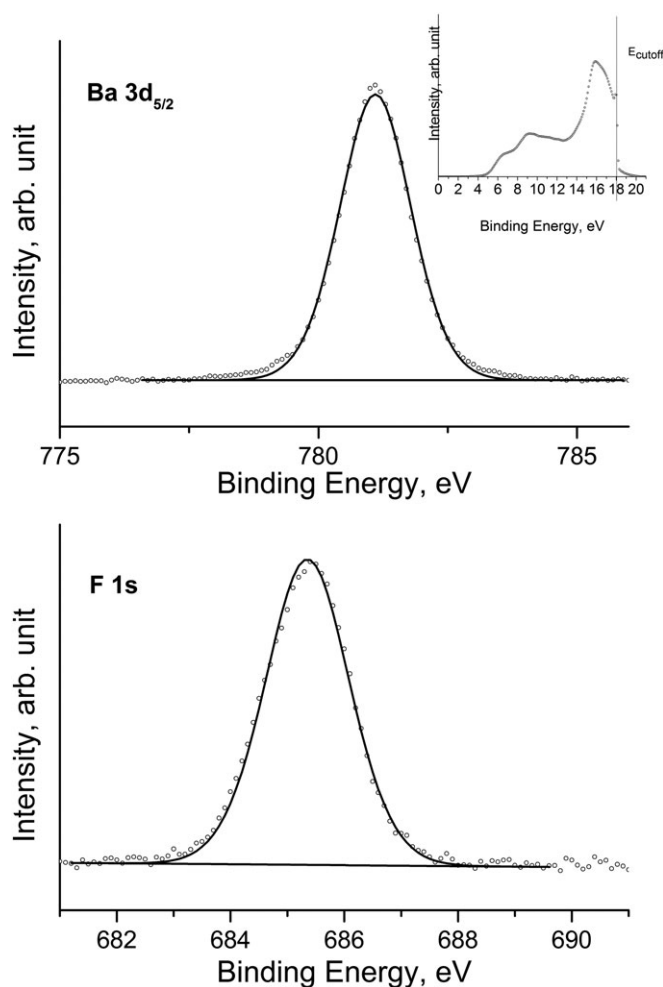

FIGURE 4   XPS and UPS (bias = 10 V) spectra of BF1 sample

typical value for oxynitrides. The obtained value of work function was high, ϕ = 4.0 eV; however, it indicates that the deposited film contributed to reduce the work function of substrate ϕ = 4.8 eV.[21] A better situation was found in AlN, where the work function of the samples AlN1 and AlN2 ϕ = 3.3-3.4 eV was comparable with LB samples and was further reduced down to 2.8-3.1 eV at higher deposition temperature of 600°C, that favors the formation of Al nitride.[20]

3.3 | Barium fluoride

The films of BaF$_2$ were tentatively deposited onto GaAs substrate in order to reduce its work function. The XPS analysis of the BaF samples revealed the presence of C, O, Ga, and As, beside of Ba and F (Table 1). The presence of C was related to the carbon contamination, which was completely removed after 30 seconds of ion sputtering. The presence of Ga 3d and As 3d signals indicates that the deposited films were very thin. In fact, their thickness was estimated to be approximately of 0.5, 0.8, and 2.0 nm for the samples BF1, BF2, and BF3, respectively. This result was correlated with increasing deposition time. The Ba 3d$_{5/2}$ peak (Figure 4) was positioned at BE = 780.3 eV, which can be assigned contemporaneously to fluoride[22] or oxide,[23] whereas a single F 1s peak was positioned at BE = 684.7 eV assigned to fluoride.[21] However, except in the thinnest film, the atomic ratio of Ba/F was not stoichiometric, indicating that also Ba was partially oxidized. The work function of the BF samples, calculated from UPS (Table 1), was independent on the thickness and unexpectedly high, even if these results are encouraging because the initial work function of GaAs ϕ = 4.77 eV[24] was significantly reduced.

Finally, the comparable values of work function for borides and nitrides were found by applying the Richardson-Dushmann's fit for the thermionic measurements. These results will be published elsewhere.

4 | CONCLUSIONS

Thin films of borides, nitrides, and fluorides with low work function were deposited by PLD and magnetron sputtering. In order to optimize the deposition parameters, the chemical composition and work function of the samples were investigated by XPS and UPS. The obtained results highlighted some critical aspects: (1) high concentration of oxygen in the films, which brought the formation of oxy-borides and oxynitrides; (2) the films were characterized by a non-stoichiometric composition with an excess of metals. Nevertheless, the work function of deposited films resulted to be sufficiently low: ϕ = 3.3-3.5 eV. These values were further reduced to ~ 2.8 eV, when the amount of borides and nitrides slightly increased. XPS results evidenced that the quality of borides and nitrides is improved by operating in ultra-high vacuum at higher temperatures, whereas the thickness of the films is directly proportional to the deposition time. In the TIPV application, in order to have an efficient energy conversion, the emitter work function must be in the range of 2.5-2.7 eV. Therefore, the obtained work function value is sufficiently compliant with the request specifications. Conversely, a work function than 2.0 eV is expected for the TIPV anode.

The barium fluoride films, although reduced the work function of the GaAs substrate (TPV cell) by 1.3-1.4 eV, are far from the requested values. Most probably, it depends from the high content of incorporated oxygen. Therefore, in the near future, it will try to act on deposition parameters to reduce the oxygen partial pressure as well as the thickness of the films, preferably monolayers.

ORCID

A. Mezzi http://orcid.org/0000-0002-2887-520X
P. Soltani http://orcid.org/0000-0003-1099-7273
S. Kaciulis http://orcid.org/0000-0002-9868-7626

REFERENCES

1. Iqbal M, Azam M, Naeem M, Khwaja AS, Anpalagan A. Optimization classification, algorithms and tools for renewable energy: a review. *Renew Sustain Energy Rev*. 2014;39:640-654.

2. Bañosa R, Manzano-Agugliarob F, Montoyab FG, Gila C, Alcaydeb A, Gómezc J. Optimization methods applied to renewable and sustainable energy: a review. *Renew Sustain Energy Rev*. 2011;15(4):1753-1766.

3. Sinha S, Chandel SS. Review of recent trends in optimization techniques for solar photovoltaic-wind based hybrid energy systems. *Renew Sustain Energy Rev*. 2015;50:755-769.

4. Bayrak F, Abu-Hamdeh N, Alnefaie KA, Öztop HF. A review on exergy analysis of solar electricity production. *Renew Sustain Energy Rev*. 2017;74:755-770.

5. Bellucci A, Calvani P, Cappelli E, et al. Preliminary characterization of ST^{2}G: Solar thermionic-thermoelectric generator for concentrating systems. *AIP Conf Proc*. 2015;1667:020007.

6. Datas A. Hybrid thermionic-photovoltaic converter. *Appl Phys Lett*. 2016;108(14):143503.

7. Hubler GK. In: Chrisey DB, Hubler GK, eds. *Pulsed Laser Deposition of Thin Films*. New York: Wiley-Interscience; 1994:327.

8. Late DJ, Date KS, More MA, et al. Some aspects of pulsed laser deposited nanocrystalline LaB6film: atomic force microscopy, constant force current imaging and field emission investigations. *Nanotechnology*. 2008;19(26):265605.

9. Jha M, Patra R, Ghosh S, Ganguli AK. Vertically aligned cerium hexaboride nanorods with enhanced field emission properties. *J Mater Chem*. 2012;22(13):6356.

10. Saitoh H, Akasaka H, Washio T, Ohkawara Y, Ohshio S, Ito H. Work function of amorphous carbon nitride with various functional groups, Part 1, No. 10. *Jpn J Appl Phys*. 2002;41:6169-6173.

11. Nemanich RJ, Baumann PK, Benjamin MC, King SW, van der Weide J, Davis RF. Negative electron affinity surfaces of aluminum nitride and diamond. *Diamond Relat Mater*. 1996;5:790-796.

12. Martinez E, Guedj C, Mariolle D, et al. Electronic and chemical properties of the TaN/a-SiOC:H stack studied by photoelectron spectroscopy for advanced interconnects. *J Appl Phys*. 2008;104(7):073708.

13. Cappelli E, Orlando S, Trucchi DM, et al. Carbon nitride films by RF plasma assisted PLD: Spectroscopic and electronic analysis. *Appl Surf Sci*. 2011;257(12):5175-5180.

14. Crociani L, Carta G, Kaciulis S, Mezzi A, Rossetto G, Zanella P. Chemical composition of magnesium boride films obtained by CVD. *Surf Interface Anal*. 2008;40(3-4):741-745.

15. Wu Y, Min G, Chen D, Zhang L, Yu H. The correlation of stoichiometry between boron-rich LaB6 targets and LaB6 films. *Ceram Int*. 2015;41(1):1005-1013.

16. Patra R, Ghosh S, Sheremet E, et al. Enhanced field emission from lanthanum hexaboride coated multiwalled carbon nanotubes: correlation with physical properties. *J Appl Phys*. 2014;116(16):164309.

17. Cappelli E, Trucchi DM, Orlando S, Bellucci A, Mezzi A, Kaciulis S. Influence of process conditions on chemical composition and electronic properties of AlN thin films prepared by ArF reactive pulsed laser deposition. *Phys Status Solidi C*. 2012;9(3-4):1053-1056.

18. Bertoti I. *Surf Coat Technol*. 2002;151/152:194.

19. Laidani N, Vanzetti L, Anderle M, Basillais A, Boulmer-Leborgne C, Perriere J. Chemical structure of films grown by AlN laser ablation: an X-ray photoelectron spectroscopy study. *Surf Coat Technol*. 1999;122(2-3):242-246.

20. Cappelli E, Trucchi DM, Kaciulis S, Orlando S, Zanza A, Mezzi A. Effect of deposition temperature on chemical composition and electronic properties of amorphous carbon nitride (a-CNx) thin films grown by plasma assisted pulsed laser deposition. *Thin Solid Films*. 2011;519(12):4059-4063.

21. Allen FG, Gobeli GW. Work function, photoelectric threshold, and surface states of atomically clean silicon. *Phys Rev*. 1962;127(1):150-158.

22. Long R, Luo J, Chen M, Wan H. Oxidative coupling of methane over BaF2-promoted rare earth oxides with variable valence. *Appl Catal A: Gen*. 1997;159(1-2):171-185.

23. Ozensoy E, Peden CHF, Szanyi J. Ba deposition and oxidation on θ-Al2O3/NiAl(100) ultrathin films. Part II: O2(g) assisted Ba oxidation. *J Phys Chem B*. 2006;110(34):17009-17014.

24. Inoue N, Higashino T, Tanahashi K, Kawamura Y. Work function of GaAs (0 0 1) surface obtained by the electron counting model. *J Cryst Growth*. 2001;227–228:123.